

RADIATION DAMPING OF SHALLOW FOUNDATIONS ON NONLINEAR SOIL MEDIUM

Jian ZHANG¹ and Yuchuan TANG²

ABSTRACT

The paper evaluates the radiation damping associated with shallow foundations sitting on linear or nonlinear soil medium. The study was motivated by the need to develop macroscopic foundation models that can realistically capture the nonlinear behaviour and energy dissipation mechanism of shallow foundations. Such model is essential to simulate the complex behaviour of structure components (e.g. shear walls, columns etc.) sitting on flexible foundations due to soil-structure interaction effects. In this study, the dynamic response of an infinitely long strip foundation resting on an elastic and inelastic half-space is investigated. The numerical analysis results presented here reveal that dynamic responses of shallow foundations strongly depend on amplitude and frequency of the input motion. In particular, the radiation damping of the system is affected by soil nonlinearity, foundation geometry and excitation frequency. The yielding of soil reduces the energy dissipation through the out going waves. As a result, the radiation damping of nonlinear soil medium is significantly lower than the elastic soil counterpart. The effects of initial elastic stiffness, yielding stress and excitation amplitude are incorporated in a nonlinearity indicator, which has shown strong correspondence to the radiation damping of the system.

Keywords: radiation damping, shallow foundation, nonlinear soil, dynamic stiffness, soil-structure interaction

INTRODUCTION

Recent earthquakes in major urban areas have underscored the need to better understand the responses of structures (e.g. bridges and buildings) to seismic actions. The responses of structures are affected by not only the nonlinear dynamic behavior of individual components (i.e. superstructure, foundations and surrounding soil) but also the complex interaction among them, i.e. the soil-structure interaction effects. During earthquakes, the foundation and surrounding soil interacts with the superstructure through changing stiffness and energy dissipation either by means of hysteretic damping or radiation damping. This interacting behaviour is often referred as inertial response in literature (Kramer 1996). The characteristics of inertial interaction can be represented by frequency dependent dynamic stiffness, which subsequently provide information on equivalent spring and dashpot constants of foundations. The kinematic response, which refers to the modification to foundation input motion due to the presence of foundations, is dealt elsewhere and is not the subject of this paper.

Various analytical models are available to describe the dynamic stiffness of shallow foundations of different shapes on elastic soil medium. The dynamic stiffness of rigid strip foundations on homogeneous elastic half-space was derived by Luco and Westmann (1972) and Hryniewicz (1981) independently. The solution for strip foundation on visco-elastic soil layer was provided by Gazetas

¹ Assistant Professor, Department of Civil & Environmental Engineering, University of California, Los Angeles, Email: zhangj@ucla.edu

² Graduate Student Researcher, Department of Civil & Environmental Engineering, University of California, Los Angeles.

and Roesset (1979) and Gazetas (1981). The dynamic stiffness of rigid circular foundation was derived by Luco and Westmann (1971) and Veletsos and Verbic (1974) for homogeneous elastic soil half-space and by Veletsos and Verbic (1973) for viscoelastic half-space. Wong and Luco (1976 and 1985) explored dynamic stiffness of rectangular foundations on either elastic soil half-space or elastic layered soil medium. Pais and Kausel (1988) proposed approximate formulas for dynamic stiffness of cylindrical and rectangular embedded foundations on homogeneous elastic soil half-space. Gazetas (1991) provided approximate formulas and charts to estimate dynamic stiffness of surface or embedded foundations on homogeneous elastic soil half-space. Most recently, Mylonakis et al. (2006) compiled an extensive set of graphs and tables for dynamic stiffness of foundations with a variety of geometries and linear soil conditions.

Despite the abundance of analytical solutions for shallow foundations on linear soil medium, very limited work has been reported on the dynamic stiffness of shallow foundations on nonlinear soil medium (Mylonakis et al., 2006). Current engineering practices rely on these linear models to estimate the dynamic response of foundations so as to derive spring and dashpot constants for use in analysis. However, the true behavior of soil is far from being linear in reality. The nonlinearity of soil has caused reduced stiffness and modified energy dissipation mechanism. As pointed out by Borja and his co-workers (Borja et al. 1993; Borja and Wu 1994), the local yielding in an otherwise homogeneous elastic soil half-space tends to reduce the radiation damping and create resonance frequencies. Their study, nevertheless, did not quantify the reduction of radiation damping resulted from soil nonlinearity.

A limited number of experiments have also been conducted on shallow foundations to evaluate their static and dynamic load-deformation behavior (Gajan et al. 2005; Faccioli et al. 2001 among others). These experimental results generally showed the nonlinear response of shallow foundations due to soil yielding and the opening and close of the gap between foundation base and underlying soil. They confirmed the need to evaluate the response of shallow foundations in the nonlinear range. However, due to the limit size of laboratory tests, these experimental results did not yield the information about the radiation damping of the system because the specimens are usually confined in a small domain. The radiation damping can be a significant portion of the energy dissipation mechanism. It often exceeds the amount of energy dissipated through hysteretic damping due to nonlinearity, especially at the higher frequencies. Therefore, it is important to accurately quantify the radiation damping when soil deforms into the nonlinear range.

In this study, finite element method is adopted to compute the dynamic response of an infinitely long strip foundation resting on an elastic and inelastic half-space. Numerical results from finite element method are compared with the theoretical solution of strip foundation on elastic half-space so as to provide guidance on choosing appropriate domain scale, mesh size and boundary conditions for correct modeling the wave propagation in a half-space. A series of parametric study is conducted to evaluate the effects of foundation width and elastic soil properties (Young's modulus and Poisson's ratio) on the dynamic stiffness of strip foundations. Closed-form formulas are developed to describe the frequency-dependent linear dynamic stiffness of strip foundation along both horizontal and vertical directions. The emphasis is then put on analyzing the dynamic response of strip foundation on nonlinear soil medium. Nonlinear constitutive model has been incorporated to exhibit yielding and kinematic hardening behavior of soil. The energy dissipation due to radiation damping is separated from that of the hysteretic damping. The numerical results show that radiation damping depends on the width of foundation, amplitude and frequency of the motion, and development of soil nonlinearity. The yield zone in soil reduces the energy dissipated through outgoing waves. As result, the radiation damping of nonlinear soil medium is significantly lower than that of elastic soil counterpart. The effects of initial stiffness, yielding stress of soil medium on dynamic stiffness of strip foundations are also investigated. The study provides valuable guidance on estimating nonlinear radiation damping parameter for soil-structure interaction analysis in engineering practices.

DYNAMIC STIFFNESS OF STRIP FOUNDATION ON ELASTIC SOIL HALF-SPACE

Consider an infinitely-long rigid strip foundation sitting on elastic soil half-space subject to harmonic excitations, as shown in Figure 1. Its dynamic stiffness can be obtained analytically. Luco and Westmann (1972) derived theoretic dynamic compliance of rigid strip foundation bonded to an elastic soil half-space using the theory of singular integral equations. An exact solution was presented for incompressible soil (Poisson's ratios $\nu=0.5$) while approximate solutions were obtained for soil of Poisson's ratio $\nu=0, 1/4, 1/3$. Hryniewicz (1981) obtained the dynamic stiffness of rigid strip foundation on an elastic half-space of Poisson's ratio $\nu=0.25$. Under a harmonic motion, the reacting forces are related to displacements by the general form shown in Eq. (1):

$$\begin{Bmatrix} P_v(t) \\ P_h(t) \end{Bmatrix} = \pi G \begin{bmatrix} c_{11} + id_{11} & 0 \\ 0 & c_{22} + id_{22} \end{bmatrix} \begin{Bmatrix} U_v(t) \\ U_h(t) \end{Bmatrix} \quad (1)$$

where G is the shear modulus of soil, $\pi G(c_{11}+id_{11})$ and $\pi G(c_{22}+id_{22})$ are the dynamic stiffness in vertical and horizontal directions respectively. The force-displacement relationship in Eq. (1) is analogous to that of a spring-dashpot system with spring constant πGc_{11} (or πGc_{22}) and dashpot coefficient $\pi Gd_{11}/\omega$ (or $\pi Gd_{22}/\omega$). The dynamic stiffness parameters $c_{11}, d_{11}, c_{22}, d_{22}$ depend on both the frequency of excitation and soil properties. The dynamic stiffness parameters are conventionally plotted against dimensionless frequency $a_0 = \omega b/\nu_s$ for a given Poisson's ratio, where b is the half-width of strip foundation and ν_s is the shear wave velocity in soil medium.

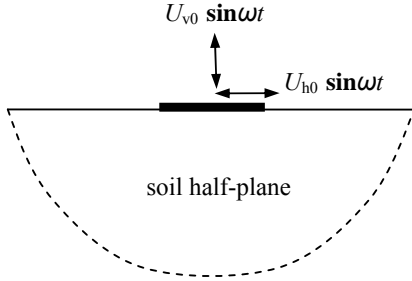


Figure 1. Foundation geometry and excitation conditions

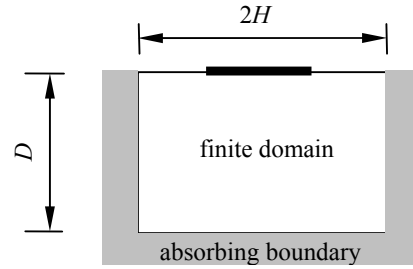


Figure 2. Finite domain and absorbing boundary

Finite element method is used in this study to conduct the dynamic analyses of strip foundation under harmonic displacement excitation in vertical and horizontal directions respectively. The soil half-space is represented by a finite domain where an absorbing boundary condition needs to be present to correctly model the outgoing waves of an infinite medium (Figure 2). Maximum element size, boundary conditions and scale of the finite domain dominate the accuracy of finite element analysis of the dynamic response of strip foundation. Judicious selection of domain scale and mesh size is required to minimize the numerical oscillations that were often observed with finite element method in this study.

The maximum element size is controlled by the shear wave length L . Kuhlemeyer and Lysmer (1973) and Lysmer et al. (1975) suggested that the maximum element size l_{\max} should satisfy

$$l_{\max} \leq \left(\frac{1}{8} \sim \frac{1}{5} \right) L \quad (2)$$

For a given finite element mesh, this rule equivalently puts an upper limit on the applicable dimensionless excitation frequency a_0 , on a specific mesh, i.e.

$$a_0 \leq \left(\frac{1}{8} \sim \frac{1}{5} \right) \frac{2\pi b}{l_{\max}} \quad (3)$$

Finite element simulation of wave propagation requires an absorbing boundary along the finite domain to allow an effective transmission of the outgoing waves. The energy dissipation mechanism of transmitting waves outwards is referred as radiation damping. Viscous damping boundary (Lysmer and Kuhlemeyer, 1969) and infinite element boundary (Lynn and Hadid, 1981) are most widely used absorbing boundaries, both of which are available in the commercial software ABAQUS Version 6.4. However, either viscous damping boundary or infinite element boundary in ABAQUS results in unexpected numerical oscillations if the selected domain is not large enough.

To avoid the uncertainty of absorbing boundary, a reliable alternative is to set up a finite domain large enough to achieve steady state response before the wave reflection at boundary contaminates the dynamic response of foundation (Borja et. al., 1993). For this purpose, the scale of the finite domain needs to satisfy

$$nTv_p \leq L_r \quad (4)$$

where L_r is the length of the shortest wave reflection path within the finite domain, v_p is the longitudinal wave velocity, T is the period of harmonic excitation, n is the number of periods from beginning of excitation which includes one full cycle of steady state response. Substituting dimensionless frequency a_0 into Eq. (4) for period T yields the lower bound on the applicable dimensionless excitation frequency

$$2n\pi \frac{b}{L_r} \cdot \sqrt{\frac{2-2\nu}{1-2\nu}} \leq a_0 \quad (5)$$

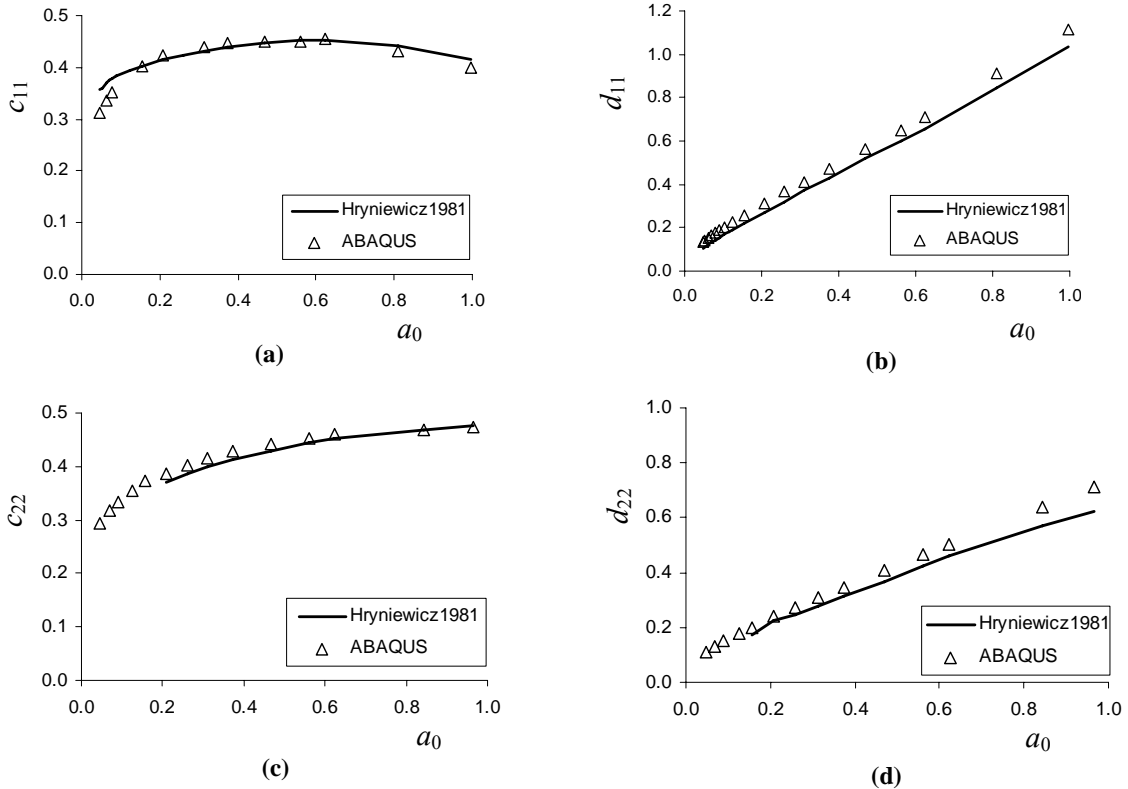


Figure 3. Dynamic stiffness parameters from FEM model: vertical (a,b) and horizontal (c,d) directions

A finite mesh of $H=250\text{m}$, $D=250\text{m}$, $l_{\max}=1.25\text{m}$ (refer to Figure 2) was set up for a strip foundation of half-width $b=1\text{m}$ on elastic soil medium of $v_s=201.5\text{m/s}$, $\nu=0.25$, $\rho=1600\text{kg/m}^3$. Eq. (5) gives lower bound of excitation frequency as $a_0 \geq 0.04$ while Eq. (3) gives upper bound of excitation frequency as $a_0 \leq 1.0$. For input frequency within this range, the numerical oscillation is well eliminated. The dynamic stiffness parameters computed by finite element method using commercial software ABAQUS are plotted in Figure 3 against the theoretical solution given by Hryniewicz (1981). The excellent agreement validates the capacity of finite element method in modeling of the foundation-soil system.

Further analyses show that the effect of either foundation half-width or Young's modulus of soil medium on dynamic stiffness parameters can be normalized by means of using dimensionless frequency a_0 as shown in Figure 4, where the effect of half-width is shown in subplots (a), (b) and effect of Young's modulus is shown in subplots (c), (d).

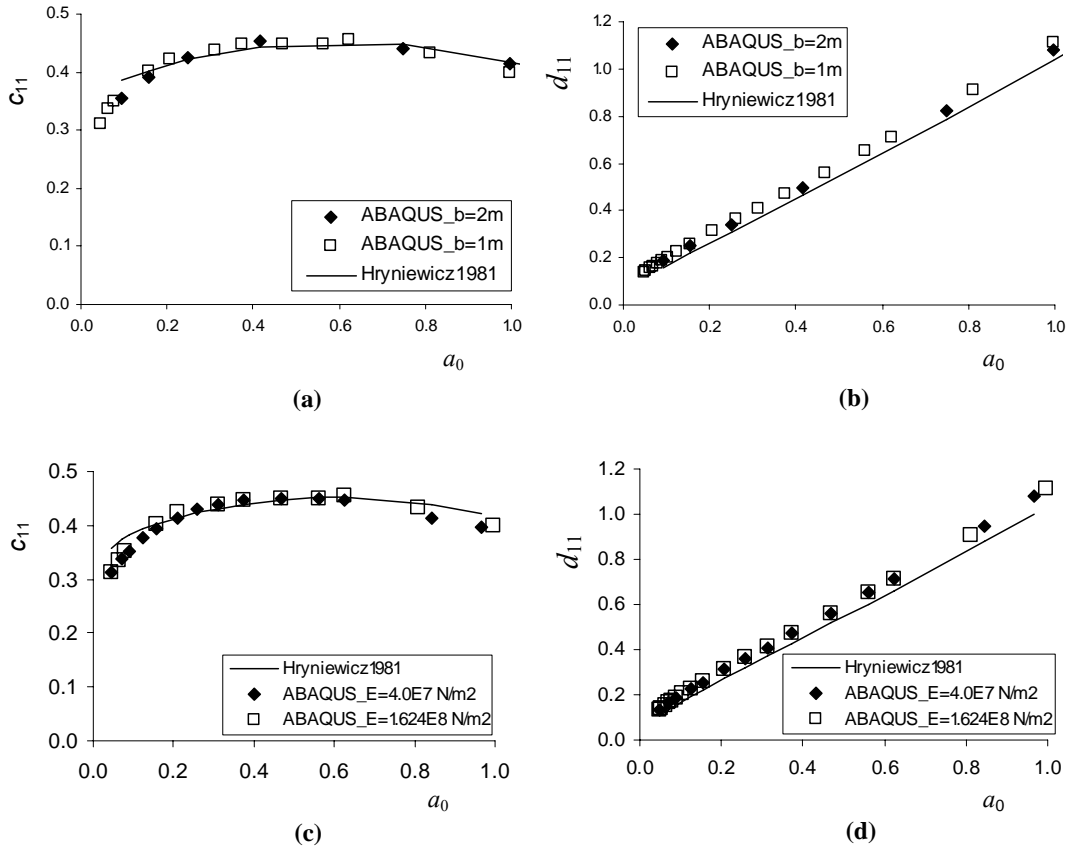


Figure 4. Effects of foundation half-width and Young's modulus of soil

Another important property of elastic soil, the Poisson's ratio ν , also affects the relationship between dimensionless dynamic stiffness parameters c_{11} , d_{11} , c_{22} , d_{22} and dimensionless frequency a_0 (Figure 5). The family of $c_{11}-a_0$ curves and $d_{11}-a_0$ curves corresponding to different Poisson's ratio describe completely the vertical dynamic stiffness of rigid strip foundation on elastic soil half-space (Figures 5a and 5b). Similarly, $c_{22}-a_0$ curves and $d_{22}-a_0$ curves represent the horizontal dynamic stiffness (Figures 5c and 5d). For practical use, the following simplified formulas are developed based on finite element analysis results:

$$c_{11} = \frac{a_0}{1.2a_0^3 - 1.1a_0^2 + 2.4a_0 + 0.04} + 0.55(\nu - 0.25) \quad (6)$$

$$d_{11} = 0.1 + (3.4\nu^2 - 0.5\nu + 0.9)a_0 \quad (7)$$

$$c_{22} = \frac{a_0}{0.45a_0^3 - 0.83a_0^2 + 2.46a_0 + 0.06} + [0.67(\nu - 0.25) + 0.01] \cdot (0.47a_0 + 0.56) \quad (8)$$

$$d_{22} = 0.1 + 0.65a_0 \quad (9)$$

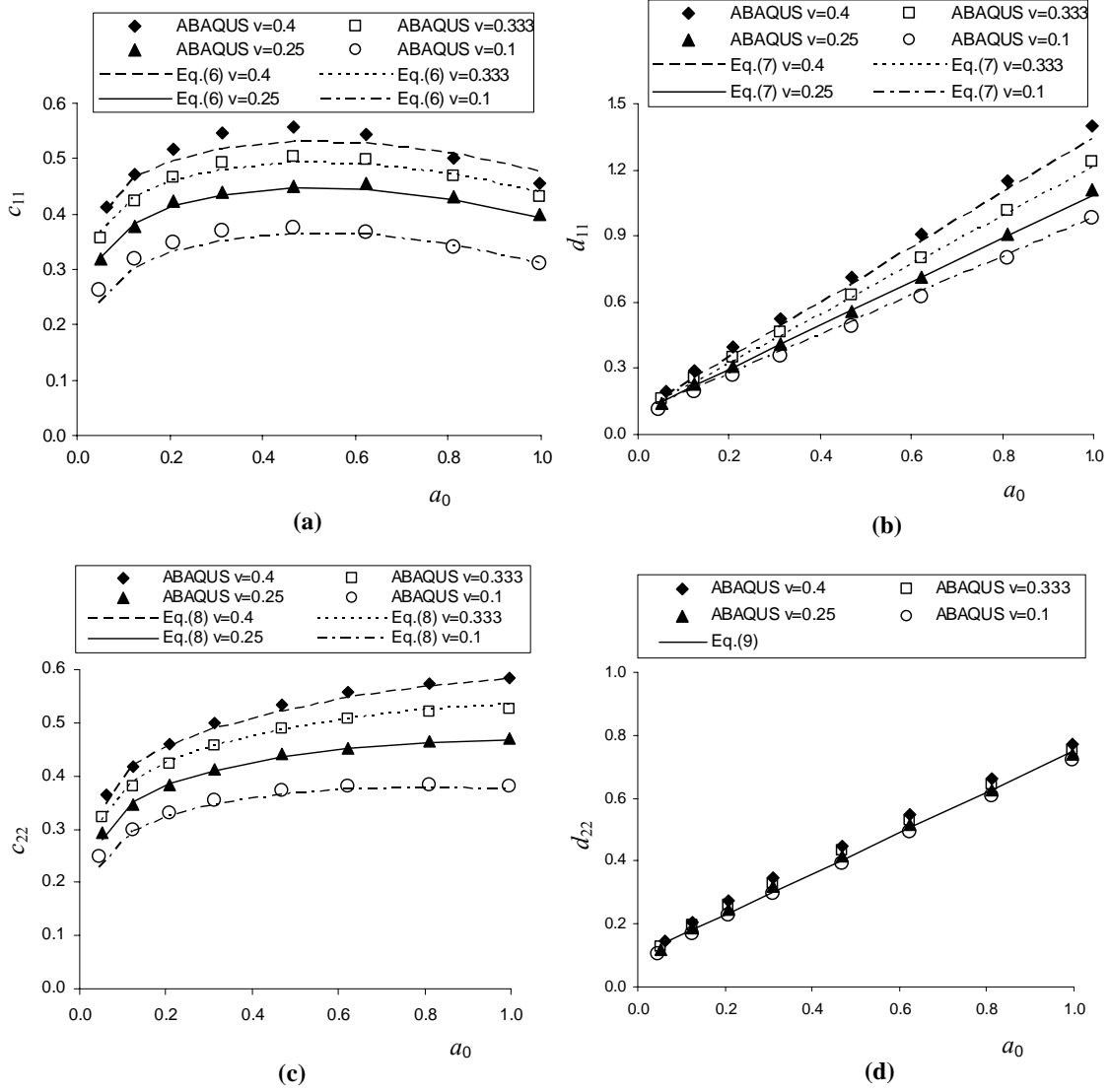


Figure 5. Effect of Poisson's ratio on dynamic stiffness along vertical (a, b) and horizontal directions (c, d)

The predicted c_{11} values with Eq. (6) and d_{11} values with Eq. (7) are compared with the finite element results in Figure 5 and showed excellent agreement. Similarly, the predicted c_{22} values with Eq. (8) and d_{22} values with Eq. (9) are also compared well with the finite element results in Figure 5 for horizontal direction. In computing the parameters c_{11} (or c_{22}) and d_{11} (or d_{22}) by finite element method, equations (10) to (12) are followed.

$$C(\omega) = \frac{W_d}{\pi \omega U_0^2} \quad (10)$$

$$d_{ii} = \frac{\omega \cdot C(\omega)}{\pi G} = \frac{a_0 \cdot C(\omega)}{\pi b \sqrt{G\rho}}, \quad i=1,2 \quad (11)$$

$$c_{ii} = \frac{P(t)/(\pi G U_0) - d_{ii} \cos(\omega t)}{\sin(\omega t)}, \quad i=1,2 \quad (12)$$

where $C(\omega)$ is equivalent dashpot value, W_d is the dissipated energy per loading cycle, U_0 is the displacement amplitude and $P(t)$ is the reaction force at time t .

RADIATION DAMPING OF STRIP FOUNDATION ON NONLINEAR SOIL HALF-SPACE

During strong earthquakes, soil often behaves nonlinearly. The plasticity experienced in soil reduces the energy dissipated through outgoing waves. As result, radiation damping of nonlinear soil is quite different from that of linear soil. Analytical derivation meets big difficulty to deal with the dynamic response of shallow foundation on nonlinear soil half-space. Alternatively, finite element modeling is an effective way to reveal the amplitude and frequency dependent nature of the foundation-nonlinear soil system.

In this section, the finite element method is used to evaluate the radiation damping of rigid strip foundation on nonlinear soil medium. It is recognized that the response of an infinitely long strip foundation on nonlinear soil medium behaves differently under static cyclic loading and dynamic harmonic excitation, as shown in Figure 6. The area within static loop accounts for hysteretic energy W_h only and is frequency independent. On the other hand, the area within dynamic loop accounts for total dissipated energy W_t through both hysteretic and radiation damping, which depends on excitation frequency. The difference between W_t and W_h is therefore the nonlinear radiation energy, W_d , which is related to nonlinear radiation dashpot coefficient C in Eq. (10) and nonlinear radiation damping parameter d_{ii} in Eq. (11).

A simple procedure has been developed to derive the model parameters for nonlinear constitutive model of soil based on widely available shear modulus reduction curves. Stress-strain relationship for simple shear can be easily obtained from shear modulus reduction curves. By applying the Masing rule to this 1D stress-strain relationship, one can obtain a cyclic loop, similar to the one shown by continuous line in Figure 7, where the soil parameters associated with Painter Street Bridge (Zhang and Makris 2002) are used. The Bouc-Wen model (Wen 1976) is then used to simulate the cyclic loop as shown by the dashed line in Figure 7. Excellent agreement can be obtained easily by adjusting the model parameters of Bouc-Wen model. This procedure allows for easy generation of cyclic behavior of different soil types so that the effects of various soil properties such as initial stiffness, yield stress and post-yielding stiffness can be evaluated.

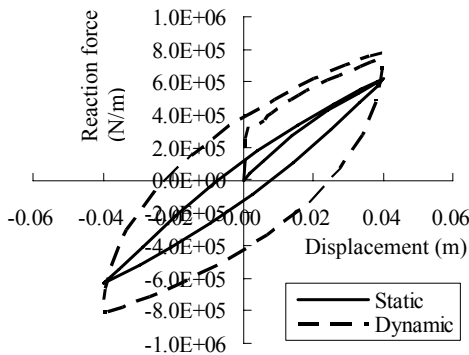


Figure 6. Static response and dynamic response of nonlinear soil

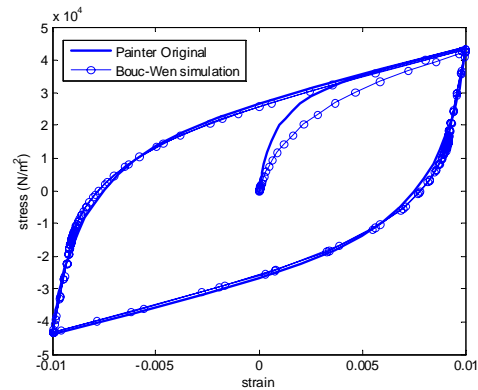


Figure 7. Bouc-Wen model for simple shear

An elasto-plastic constitutive model of von Mises yield criterion and nonlinear kinematic hardening rule in ABAQUS was selected to simulate nonlinear soil material. The elasto-plastic material model was defined by a few representative points on the steady-state cyclic loop, e.g. the one given by Bouc-Wen model in Figure 7. Figure 8 compares the response of a single plane-strain element subjected to simple shear predicted by ABAQUS and the input curve based on Masing rule. The input to ABAQUS was done by picking up four representative points from the Bouc-Wen loop in Figure 7 and the program computes the nonlinear kinematic hardening parameters automatically. The excellent agreement shown on Figure 8 verifies this procedure. A number of simulations (not shown here) have also been conducted to verify that the possibility of using this model to predict the response of other soil types. With the careful selection of nonlinear kinematic hardening parameters, the model is able to predict the soil behavior and energy dissipation with reasonable accuracy. Nevertheless, this model is not intended to be used for liquefiable soil.

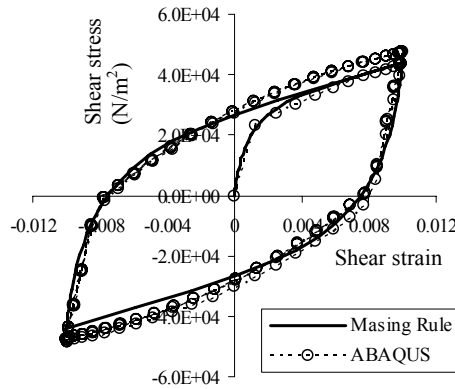


Figure 8. ABAQUS simulation of simple shear

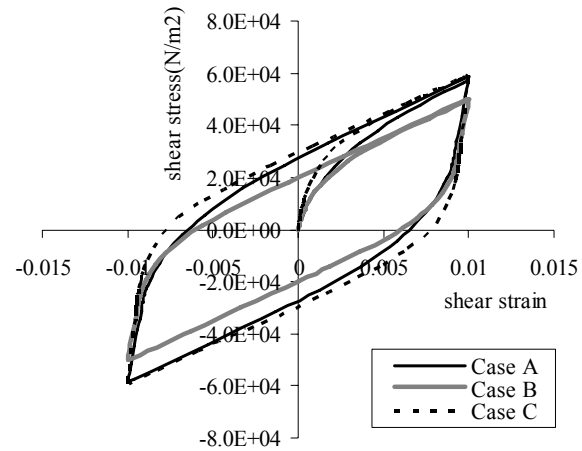


Figure 9. Three distinctive soil models for parametric study

Parametric studies are performed on three different soil models to evaluate the effects of initial stiffness and yielding stress on dynamic stiffness of the strip foundation on nonlinear soil medium. Three Bouc-Wen simple shear loops, Cases A, B and C, were generated for this purpose (Figure 9). Case A differs from Case B only in yield shear stress τ_y , which is 3.0×10^4 N/m² and 2.1×10^4 N/m² for Case A and B respectively. Case A differs from Case C only in shear modulus G , which is 6.0×10^7 N/m² and 1.0×10^8 N/m² for Case A and C respectively. Poisson's ratio 0.25 is specified for all three soil material cases.

Besides Eq. (3) and Eq. (5), the possible development of plasticity in soil medium should also be taken into account to set up finite element mesh for nonlinear dynamic analysis. Development of plasticity results in smaller wave velocity, which requires finer mesh in the region where soil yields. Following all the restrictions and taking advantage of symmetry or anti-symmetry, two plane strain finite element meshes was set up for different excitation frequency ranges. For frequency range 0.4Hz~1.0Hz, the mesh is of $H=D=1800$ m, $l_{\max}=10$ m and has uniform finer rectangular elements of $0.1\text{m} \times 0.1\text{m}$ within the $12\text{m} \times 12\text{m}$ region near the foundation. For frequency range 1.0Hz~3.0Hz, the mesh is of $H=D=700$ m, $l_{\max}=3$ m and has uniform finer rectangular elements of $0.1\text{m} \times 0.1\text{m}$ within the $14\text{m} \times 14\text{m}$ region near the foundation.

Effect of soil density is discussed at first. Dynamic finite element analyses of a strip foundation of half-width $b=1$ m on soil medium of material Case A under vertical harmonic excitation $U(t) = 0.02 \sin \omega t$ (meter) were performed with different soil densities $\rho=800\text{kg/m}^3$, 1600kg/m^3 , 2000kg/m^3 respectively. Figure 10 plots d_{11} vs. a_0 curves for different soil density. It shows that soil density does not affect the dimensionless nonlinear radiation damping parameter. This finding does

not contradict the experimental evidence that the soil density affects the response of soil. Instead, its effect is normalized through the dimensionless parameter a_0 hence does not show up in the plot.

It is anticipated that the amplitude of displacement excitation will affect the development of nonlinearity in soil medium. As a result, nonlinear radiation damping is displacement-amplitude dependent, as it differs from linear radiation damping. Figure 11 plots the nonlinear radiation damping for soil material Case A with density of $\rho=1600\text{kg/m}^3$ and different combinations of foundation half-width b and displacement amplitude U_0 . It is observed from Figure 11 that the nonlinear radiation damping parameter depends on the ratio U_0/b rather than U_0 itself. Analyses with soil material Cases B and C reveal the similar trend. Larger U_0/b results in more nonlinearity in soil, which leads to smaller radiation damping due to outgoing waves.

Besides the ratio U_0/b , soil properties also affect the nonlinear behavior of strip foundation. Figure 12 shows the static responses of a strip foundation of $b=2\text{m}$ under vertical cyclic displacement of amplitude 0.04m with soil material Case A, B, C respectively. Case A and Case B lead to different yield displacement in foundation behavior. Case A and Case C lead to different initial stiffness in foundation behavior.

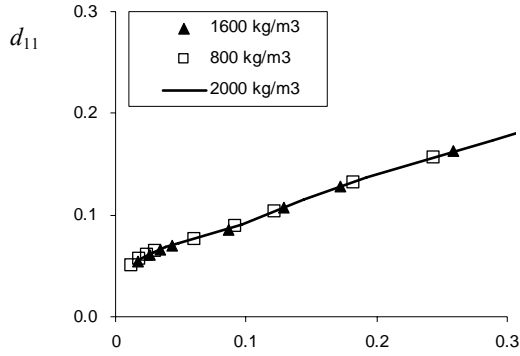


Figure 10. Effect of soil density

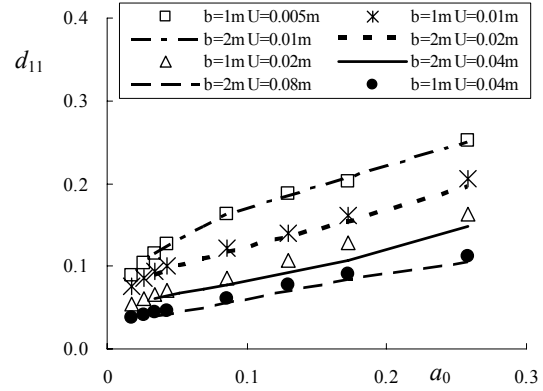


Figure 11. Effect of ratio U_0/b

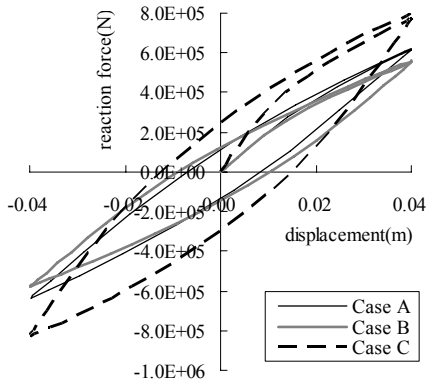


Figure 12. Static cyclic behavior of foundation

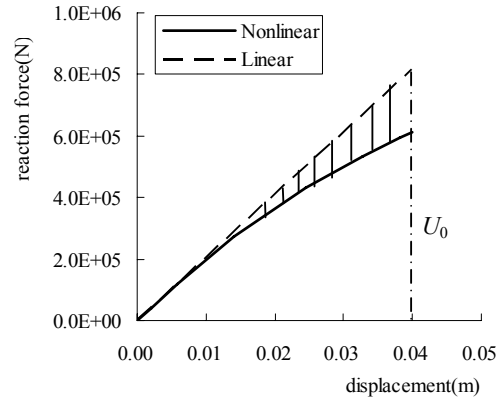


Figure 13. Static behavior of foundation

Static analysis of the strip foundation on nonlinear soil with finite element method gives a nonlinear initial loading curve as shown in Figure 13. Assuming small deformation, the initial linear portion of the nonlinear curve can be extended to any displacement level to get the linear counterpart. The deviation of the nonlinear curve from its linear counterpart indicates the degree of nonlinearity in the soil medium. To quantify the degree of nonlinearity in soil medium under displacement excitation at foundation, nonlinearity indicator δ is defined as

$$\delta = \frac{W_{linear} - W_{nonlinear}}{W_{linear}} \times 100\% \quad (13)$$

where W_{linear} is the work done along linear loading path from the origin to U_0 , and $W_{nonlinear}$ is the work done along nonlinear loading path from origin to U_0 . The shaded area in Figure 13 illustrates the numerator in Eq. (13). Essentially, the nonlinear indicator covers both the effect of U_0/b and the effect of nonlinear soil properties at a global level.

Static finite element analyses were performed to get nonlinearity indicators for the combinations of different soil material cases and U_0/b ratios as listed in Table 1. Larger nonlinearity indicator indicates more nonlinearity in soil. Nonlinear dynamic analyses with finite element method gave nonlinear radiation damping parameters of the combinations of different soil material cases and U_0/b ratios as plotted in Figure 14. Referring to Table 1, Figure 14 reveals that the radiation damping decreases monotonically with the development of nonlinearity in soil medium i.e. increase of nonlinearity indicator. The results show the great promise of using the nonlinearity indicator as quantifying parameter for radiation damping of strip foundation on nonlinear soil medium.

Table 1. Nonlinearity indicators for different combinations

	$U_0/b=0.001$	$U_0/b=0.005$	$U_0/b=0.01$	$U_0/b=0.02$
Soil Case A	—	0.43%	4.00%	14.87%
Soil Case B	—	1.03%	8.33%	21.77%
Soil Case C	0.07%	3.16%	15.01%	31.62%

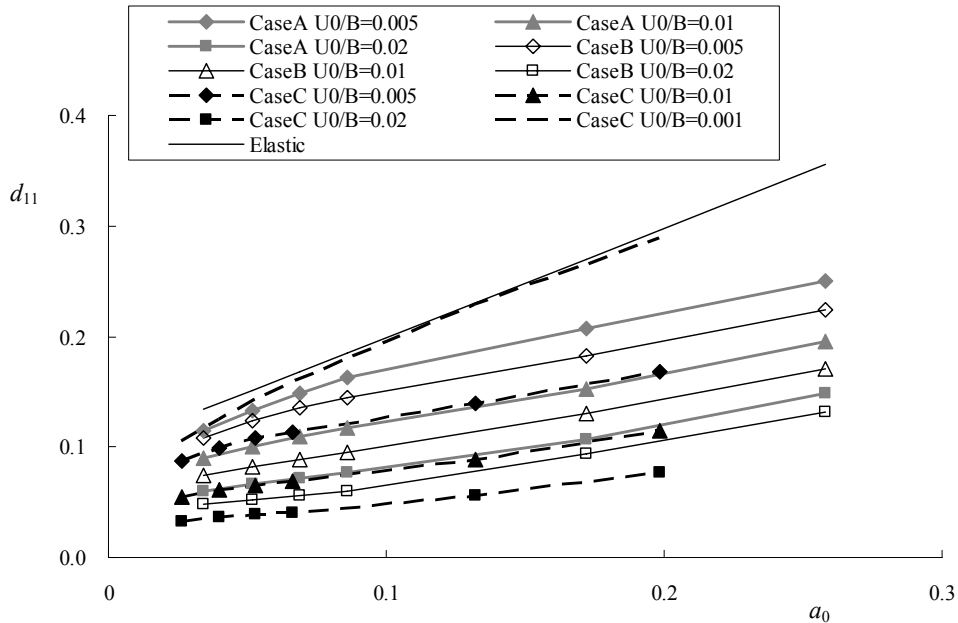


Figure 14. Nonlinear radiation damping

CONCLUSIONS

In this study, the dynamic stiffness of strip foundation on linear and nonlinear soil medium is analyzed by finite element method. The numerical results from FEM are compared with theoretical solution of strip foundations on elastic half-space. Special attentions are paid to choosing appropriate domain scale, mesh size and boundary conditions so that the wave propagation in an infinite domain can be correctly modeled. Excellent agreement between finite element analysis and theoretical results can be achieved by judicious selection of domain scale and mesh size. Closed-form formulas are then developed to describe the spring and dashpot constants of dynamic stiffness as function of frequency as well as their dependency on foundation width, Young's modulus and Poisson's ratio. The analysis of strip foundation on nonlinear soil medium shows that energy dissipation depends on the amplitude of the motion and frequency. The plasticity in soil reduces the energy dissipated through outgoing waves. As result, the radiation damping of nonlinear soil is significantly lower than the elastic soil counterpart. The study investigated the effects of initial elastic stiffness, yielding stress and post-yielding stiffness on radiation damping. A nonlinearity indicator is developed and has been shown to directly relate to the reduction of radiation damping due to soil yielding. The findings are important to dynamic responses of structures supported on shallow foundations since the reduced radiation damping at foundation level will result in increased structural response.

ACKNOWLEDGEMENTS

Partial financial support for this study was provided by National Science Foundation under grant NEESR-0421577.

REFERENCES

- Borja, R.I., Wu, W-H. and Smith, H.A. (1993), "Nonlinear response of vertically oscillating rigid foundations", *Journal of Geotechnical Engineering*, ASCE, 119(5):893-911.
- Borja, R.I. and Wu, W-H. (1994), "Vibration of foundations on incompressible soils with no elastic region", *Journal of Geotechnical Engineering*, ASCE, 120(9):1570-1592.
- Faccioli, E., Paolucci, R., and Vivero, G. (2001), "Investigation of seismic soil-footing interaction by large scale cyclic tests and analytical models", *Proc. 4th International Conference on Recent Advances in Geotechnical Earthquake Engineering and Soil Dynamics*, pp. 26-31, San Diego, CA.
- Gajan, S., Kutter, B. L., Phalen, J.D., Hutchinson, T.C. and Martin, G.R. (2005), "Centrifuge modeling of load-deformation behavior of rocking shallow foundations", *Soil Dynamics and Earthquake Engineering*, 25:773-783.
- Gazetas, G. and Roesset, J.M. (1979), "Vertical vibrations of machine foundations", *Journal of the Geotechnical Engineering Division*, ASCE, 105(GT12):1435-1454.
- Gazetas, G. (1981), "Strip foundations on cross-anisotropic soil layer subjected to static and dynamic loading", *Geotechnique*, 31(2):161-179.
- Gazetas, G. (1991), "Formulas and charts for impedances of surface and embedded foundations", *Journal of Geotechnical Engineering*, ASCE, 117(9):1361-1381.
- Hryniewicz, Z. (1981), "Dynamic response of a rigid strip on an elastic half-space", *Computer Methods in Applied and Mechanical Engineering*, 25(3):355-364.
- Kramer, S. (1996), *Geotechnical earthquake engineering*, Prentice Hall, Upper Saddle River, NJ.

- Kuhlemeyer, R.L. and Lysmer, J. (1973), "Finite element method accuracy for wave propagation problems", *Journal of Soil Mechanics and Foundations Division*, ASCE, 99(SM5):421-427.
- Luco, J.E. and Westmann R.A. (1971), "Dynamic response of circular footings", *Journal of Engineering Mechanics Division*, ASCE, 97(EM5):1381-1395.
- Luco, J.E. and Westmann R.A. (1972), "Dynamic response of a rigid footing bonded to an elastic half space", *Journal of Applied Mechanics*, ASME, 39(2):527-534.
- Lysmer, J. and Kuhlemeyer R.L. (1969), "Finite dynamic model for infinite media", *Journal of Engineering. Mechanics Division*, ASCE, 95(4):859-877.
- Lysmer, J., Udaka, T., Tsai, C.F., and Seed, H.B. (1975), "FLUSH: a computer program for approximate 3-D analysis of soil-structure interaction problems", *Report EERC 75-30*, Earthquake Engineering Research Center, University of California, Berkeley, 83pp.
- Lynn, P.P. and Hadid H. A. (1981), "Infinite elements with $1/rn$ type decay", *International Journal for Numerical Methods in Engineering*, 17(3):347-355.
- Mylonakis, G., Nikolaou, S. and Gazetas, G. (2006), "Footings under seismic loading: analysis and design issues with emphasis on bridge foundations", *Soil Dynamics and Earthquake Engineering*, 26(9):824-853.
- Pais, A. and Kausel, E. (1988), "Approximate formulas for dynamic stiffnesses of rigid foundations", *Soil Dynamics and Earthquake Engineering*, 7(4):213-227.
- Veletsos, A.S. and Verbic, B. (1973), "Vibration of viscoelastic foundations", *Earthquake Engineering and Structural Dynamics*, 2(1):87-102.
- Veletsos, A.S. and Verbic, B. (1974), "Basic response functions for elastic foundations", *Journal of Engineering Mechanics*, ASCE, 100(EM2):189-202.
- Wen, Y-K. (1976), "Method for random vibration of hysteretic systems", *Journal of Engineering Mechanics Division*, ASCE, 102(EM2): 249-263.
- Wong, H.L. and Luco, J.E. (1976), "Dynamic response of rigid foundations of arbitrary shape", *Earthquake Engineering and Structural Dynamics*, 4(6):579-587.
- Wong, H.L. and Luco, J.E. (1985), "Tables of Impedance Functions for square foundations on layered media", *Soil Dynamics and Earthquake Engineering*, 4(2):64-81.
- Zhang, J. and Makris, N. (2002), "Kinematic response functions and dynamic stiffnesses of bridge embankments", *Earthquake Engineering and Structural Dynamics*, 31(11):1933-1966.